ISSN 1070-3632, Russian Journal of General Chemistry, 2011, Vol. 81, No. 7, pp. 1547–1554. © Pleiades Publishing, Ltd., 2011.
Original Russian Text © K.P. Balashev, M.V. Puzyk, E.V. Ivanova, 2011, published in Zhurnal Obshchei Khimii, 2011, Vol. 81, No. 7, pp. 1199–1207.

# Optical and Electrochemical Properties of Cyclometallated Rh(III) and Pd(II) Complexes Based on Phenyl-Substituted Pyrazole, Pyridine, and Pyrimidine with Ethylenediamine, 2,2'-Bipyridine, and 1,10-Phenanthroline

**K. P. Balashev, M. V. Puzyk, and E. V. Ivanova**

*Herzen Russian State Pedagogical University, nab. r. Moiki 48, St. Petersburg, 191186 Russia*
*e-mail: balashevk@mail.ru*

Received January 20, 2011

**Abstract**—Electrochemical and optical properties of cyclometallated Rh(III) and Pd(II) complexes based on phenyl-substituted pyrazole, pyridine, and pyrimidine with ethylenediamine, 2,2'-bipyridine, and 1,10-phenanthroline chelating ligands were investigated. One-electron reduction waves of the complexes were assigned to ligand-centered processes of electron transfer on π* orbitals of heterocyclic chelating and cyclometallated ligands, whereas irreversible oxidation waves, to the processes involving a mixed phenyl-metal π/d orbital. The long-wave absorption band results from by the spin-allowed optical transition between π/d-HOMO and a π* orbital of a cyclometallated ligand. The character of the optical transition responsible for low-temperature (77 K) phosphorescence of the complexes is defined by the ratio of the energy gap between π* orbitals of chelating and cyclometallated ligands and by the energy of the singlet–triplet splitting of electron-excited states.

**DOI:** 10.1134/S1070363211070231

The specificity of the electronic structure of cyclometallated complexes of platinum metals combining properties of coordination and organometallic compounds defines wide prospects of the use of photosensitive complexes: luminescent labels of biological materials [1], optical sensors [2], emitters in organic light-emitting diodes [3], materials with liquid-crystal [4] and photoreactive [5] properties, and components of photocatalytic systems for solar energy conversion into chemical or electrical energy [6]. The study of the influence of the nature of heterocyclic cyclometallated and chelating ligands on optical and electrochemical properties of various Ir(III) and Pt(II) complexes made it possible to offer methods of their directional modification for increasing efficiency of light-emitting diodes of a new generation [7]. Cyclometallated complexes of Rh(III) and Pd(II) are investigated much less. It limits a possibility of developing common conceptions concerning directional modification of optical and electrochemical properties of cyclometallated complexes by variation of the nature of ligands and metals.

In the present work we have considered the influence of the nature of cyclometallating and other chelating ligands on optical and electrochemical properties of mixed-ligand complexes $[Rh(C^N)_2(N^N)]^+$, $[Pd(C^N)(N^N)]^+$, and $[(Pd(N^N))_2(\mu\text{–}C^N\text{–}N^C)]^{2+}$ [(C^N) are deprotonated forms of 1-phenylpyrazole (**I**), 2-phenyl (**II**), and 4,6-diphenylpyrimidine (**III**); $(C^N\text{–}N^C)^{2-}$ is the bisdeprotonated form of 4,6-diphenylpyrimidine (**IV**); (N^N), ethylenediamine (**V**), 2,2'-bipyridine (**VI**), and 1,10-phenanthroline (**VII**)].

Within the limits of the localized molecular orbitals model [8] optical and electrochemical characteristics of compounds are classified according to the presumable localizations of molecular orbitals participating in a photo- and electro-stimulated electronic transition. For metallocomplex compounds metal- and ligand-centered intraligand optical transitions and ligand–ligand, metal–ligand, and ligand-metal charge-transfer transitions are distinguished. Presuming that Koopman's theorem [9] is valid, we can expect that the highest occupied (HOMO) and the lowest unoccupied

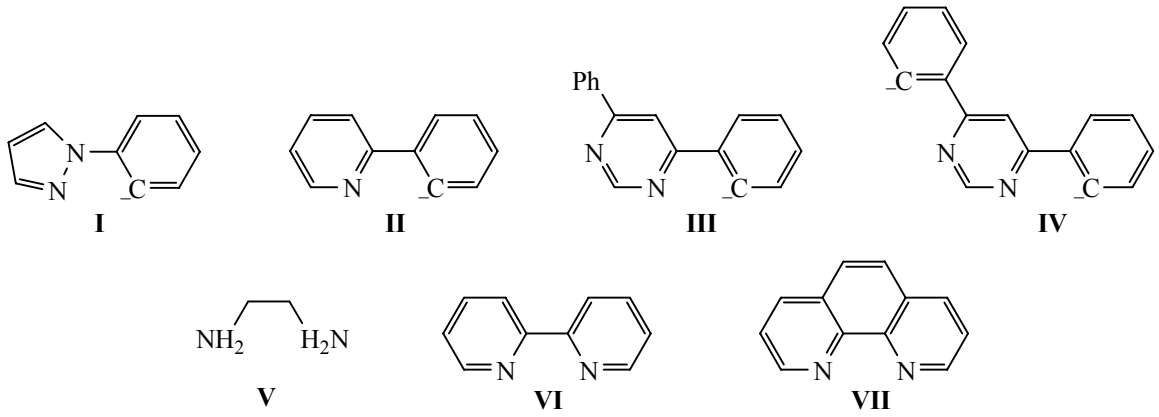


(LUMO) orbitals responsible for low-energy optical transitions and electrochemical properties of complexes are similar.

Optical and electrochemical properties of free phenyl-substituted heterocyclic ligands are defined (Table 1) by electron-transfer processes involving π and π* orbitals preferentially localized on pyrazole, pyridine, and pyrimidine components. The decrease in the energy of delocalization of pyridine and pyrimidine π* orbitals in comparison with pyrazole leads both to a red bathochromic shift of spin-allowed and spin-forbidden optical transitions in absorption and phosphorescence spectra and to an anode shift of a reduction potential. The deprotonation of the phenyl component of ligands results in lowering the π*-orbital energy and gives rise to a red shift of optical transitions by ~10 nm [10.] Chelating heterocyclic ligands (**VI** and **VII**) are also characterized by the presence of photo- and electro-stimulated electron-transfer processes involving π- and π*-orbitals. A complex formation results in lowering energy of optical π–π* transitions by a value of no less than 1000 $cm^{-1}$ [11] and in an anode shift of the ligand-centered reduction potential [12], the value of which depends on the effectiveness of a ligand–metal donor–acceptor interaction.

Results of studying optical and electrochemical characteristics of complexes (Tables 2 and 3) show that they considerably differ from those of ligands (Table 1) depending on the nature of metals and ligands. Electronic absorption spectra of complexes, alongside with a typical (<1000 $cm^{-1}$) red shift of intraligand $^1(\pi–\pi^*)$ optical transitions, are characterized by the presence of absorption bands in the region of longer waves, the energy position and extinction coefficient of which considerably depend on the ligand and metal nature. Spectra of low-temperature (77 K) phosphorescence of complexes and time (τ) of its quenching also considerably vary as the nature of ligands and metal is varied. Voltammograms of reduction of the complexes are characterized by the presence of quasi-reversible one-electron waves

**Table 1.** Optical and electrochemical parameters of heterocyclic ligands

| Ligand no. | Absorption (293 K) | | Emission (77 K) | | Reduction potential | |
|---|---|---|---|---|---|---|
| | $\lambda_{max}$, nm ($\varepsilon\times10^3$, $l\ mol^{-1}\ cm^{-1}$) | optical transition | $\lambda_{max}$, nm (τ, μs) | optical transition | $-E$, V[a] | MO |
| $\mathbf{I}_H$ [13] | 255 (15.1)[b] | $^1(\pi–\pi^*)$ | 378 (>$10^5$)[f] | $^3(\pi–\pi^*)$ | <3.0 | – |
| $\mathbf{II}_H$ [14] | 274 (8.9)[c] | $^1(\pi–\pi^*)$ | 430 (>$10^5$)[f] | $^3(\pi–\pi^*)$ | 2.5[i] | π* |
| $\mathbf{III}_H$ | 300 sh (3.6)[d] | $^1(\pi–\pi^*)$ | 423 (>$10^5$)[g] | $^3(\pi–\pi^*)$ | 2.45[i] | π* |
| **VI** [13] | 281 (10.0)[e] | $^1(\pi–\pi^*)$ | 436 ($1\times10^6$)[e] | $^3(\pi–\pi^*)$ | 2.55 | π* |
| **VII** | 262 (10.0)[c] | $^1(\pi–\pi^*)$ | 459[h] [15] | $^3(\pi–\pi^*)$ | 2.51 | π* |

[a] $(CH_3)_3NCO(H)$, 293 K. [b] $CH_2Cl_2$. [c] EtOH–$H_2O$. [d] $CH_3CN$. [e] MeOH–$H_2SO_4$. [f] $C_3H_5CN$. [g] $(CH_3)_3NCO(H)$–$C_6H_5CH_3$, 1:1. [h] $Et_2O$. [i] A current peak potential of irreversible wave at a potential scanning rate of 100 mV $s^{-1}$.

**Table 2.** Optical and electrochemical characteristics of $[Rh(C^N)_2(N^N)]^+$ complexes

| (C^N), (N^N) | Absorption[a] | | Emission[b] | | Oxidation[a] and reduction[c] | | | |
|---|---|---|---|---|---|---|---|---|
| | $\lambda_{max}$, nm ($\varepsilon\times10^3$, l mol$^{-1}$ cm$^{-1}$) | optical transition | $\lambda_{max}$, nm ($\tau$, μs) | optical transition | $E_p$, V | MO | $-E_{1/2}$, V | MO |
| **I, V** | 324 (2.3) | $^1(\pi_I/d–\pi^*_I)$ | <400 | – | 1.04 | $\pi_I/d$ | <2.5 | – |
| **I, VI** | 324 sh (0.9) | $^1(\pi_I/d–\pi^*_I)$ | 440 (320) | $^3(\pi_{VI}–\pi^*_{VI})$ | 1.17 | $\pi_I/d$ | 1.76 | $\pi^*_{VI}$ |
| **I, VII** | 320 sh (1.3) | $^1(\pi_I/d–\pi^*_I)$ | 437 ($7.9\times10^3$) | $^3(\pi_{VII}–\pi^*_{VII})$ | 1.21 | $\pi_I/d$ | 1.73 | $\pi^*_{VII}$ |
| **II, VI** | 364 (0.73) | $^1(\pi_{II}/d–\pi^*_{II})$ | 454 (180)[d] | $^3(\pi_{II}/d–\pi^*_{VI})$ | 1.20 | $\pi_{II}/d$ | 1.84[f] | $\pi^*_{VI}$ |
| | | | | | | | 2.49[f] | $\pi^*_{II}$ |
| | | | | | | | 2.76[f] | $\pi^*_{II}$ |
| **II, VII** | 370 sh (0.8)[d] | $^1(\pi_{II}/d–\pi^*_{II})$ | 454 (190)[e] | $^3(\pi_{II}/d–\pi^*_{VII})$ | 1.07 | $\pi_{II}/d$ | 1.86 | $\pi^*_{VII}$ |
| | | | | | | | 2.55 | $\pi^*_{II}$ |
| | | | | | | | 2.85 | $\pi^*_{II}$ |
| **III, V** | 410 (3) | $^1(\pi_{III}/d–\pi^*_{III})$ | 483 (10) | $^3(\pi_{III}/d–\pi^*_{III})$ | 1.09 | $\pi_{III}/d$ | 1.90 | $\pi^*_{III}$ |
| | | | | | | | 2.10 | $\pi^*_{III}$ |
| **III, VI** | 395 (6.4) | $^1(\pi_{III}/d–\pi^*_{III})$ | 464 (13) | $^3(\pi_{III}/d–\pi^*_{VI})$ | 1.30 | $\pi_{III}/d$ | 1.69 | $\pi^*_{VI}$ |
| | | | | | | | 1.92 | $\pi^*_{III}$ |
| **III, VII** | 393 (10.5) | $^1(\pi_{III}/d–\pi^*_{III})$ | 463 (14) | $^3(\pi_{III}/d–\pi^*_{VII})$ | 1.32 | $\pi_{III}/d$ | 1.68 | $\pi^*_{VII}$ |
| | | | | | | | 1.94 | $\pi^*_{III}$ |

[a] $CH_3CN$, 293 K. [b] $(CH_3)_3NCO(H)–C_6H_5CH_3$, 1:1, 77 K. [c] $(CH_3)_3NCO(H)$, 293 K. [d] EtOH–MeOH, 4:1, 77 K. [e] $C_3H_5CN$. [f] $CH_3CN$, –40°C.

connected with sequential ligand-centered processes of electron transfer, which points to a preferential LUMO localization on π*-orbitals of heterocyclic ligands in the complex composition. Voltammograms of oxidation of the complexes, on the contrary, are of irreversible nature.

The ligand-centered nature of one-electron waves of the reduction of complexes with chelating ethylenediamine (En) allows us to assign their LUMO to an orbital preferentially localized on the cyclometallated ligand ($\pi^*_{C^N}$). The presence of two cyclometallated ligands in the internal sphere of the complex with 4,6-diphenylpyrimidine $[Rh(C^N)_2En]^+$ defines the presence of two waves of its reduction ($E^1_S$ and $E^2_S$), the difference between their half-wave potentials ($E_{1/2}$ 200 mV) being in agreement with the selective reduction of cyclometallated 2-phenylpyridine (ppy) in the composition of $[Ir(ppy)_3]$ [16].

$$[Rh(C^N)_2En]^+ + e^- \leftrightarrow [Rh(C^N)(C^N{}^-)En] \qquad E^1_S,$$

$$[Rh(C^N)(C^N{}^-)En] + e^- \leftrightarrow [Rh(C^N{}^-)_2En]^- \qquad E^2_S.$$

According to the elevated energy of $\pi^*_{C^N}$-orbitals of pyrazole, as compared with pyridine and pyrimidine, irrespective of the metal nature, the reduction potentials of all complexes based on 1-phenylpyrazole and ethylenediamine are outside the stability of the dimethyl formamide solvent. The anode shift of the potential of ligand-centered reduction of mononuclear complexes based on phenyl-substituted pyridine and pyrimidine in relation to the free ligands (Table 1) is practically independent of the metal nature and is equal to 0.3 and 0.6 V, respectively. The presence of two metal centers in the structure of binuclear complexes $\{[Pd(N^N)]_2(\mu–C^N–N^C)\}^{2+}$ results in the additional anode 0.3 V shift of the reduction potential of biscyclometallated 4,6-diphenylpyrimidine as compared with mononuclear complexes.

The substitution of heterocyclic diimine ligands for ethylenediamine leads to the presence of a series of one-electron ligand-centered waves in the reduction voltammograms of mono- and binuclear complexes resulted from sequential processes of electron transfer on π*-orbitals localized on cyclometallated $\pi^*_{C^N}$-and chelating $\pi^*_{N^N}$-ligands. Voltammograms of mononuclear complexes are characterized by the presence of additional anode-displaced wave assigned to the electron transfer on $\pi^*_{N^N}$-orbitals of a diimine ligand,

**Table 3.** Optical and electrochemical characteristics of the complexes $[Pd(C^N)(N^N)]^+$ and $[(Pd(N^N))_2(\mu\text{-}C^N\text{-}N^C)]^{2+}$

| (C^N), (N^N) | Absorption[a] | | Emission[b] | | Oxidation[a] and reduction[c] | | | |
|---|---|---|---|---|---|---|---|---|
| | $\lambda_{max}$, nm ($\varepsilon\times10^3$, $l\ mol^{-1}\ cm^{-1}$) | optical transition | $\lambda_{max}$, nm ($\tau$, μs) | optical transition | $E_p$, V | MO | $-E_{1/2}$, V | MO |
| $[Pd(C^N)(N^N)]^+$ | | | | | | | | |
| **I, V** | 304 (3.4) | $^1(\pi_I/d–\pi^*_I)$ | <400 | – | 0.9 | $\pi_I/d$ | <2.5 | – |
| **I, VI** | 320 sh (2) | $^1(\pi_I/d–\pi^*_I)$ | 477 (43) | $^3(\pi_I/d–\pi^*_{VI})$ | 1.0 | $\pi_I/d$ | 1.63 | $\pi^*_{VI}$ |
| **I, VII** | 324 (1.4) | $^1(\pi_I/d–\pi^*_I)$ | 475 (22) | $^3(\pi_I/d–\pi^*_{VII})$ | 0.9 | $\pi_I/d$ | 1.62[d] | $\pi^*_{VII}$ |
| **II, V** | 350 sh (4)[c] | $^1(\pi_{II}/d–\pi^*_{II})$ | 462 (320) | $^3(\pi_{II}/d–\pi^*_{II})$ | 1.0 | $\pi_{II}/d$ | 2.19[d] | $\pi^*_{II}$ |
| **II, VI** | 337 (4.3) | $^1(\pi_{II}/d–\pi^*_{II})$ | 463 (210) | $^3(\pi_{II}/d–\pi^*_{II})$ | 0.9 | $\pi_{II}/d$ | 1.64 | $\pi^*_{VI}$ |
| | | | | | | | 1.95[d] | $\pi^*_I$ |
| **II, VII** | 355 sh (3)[c] | $^1(\pi_{II}/d–\pi^*_{II})$ | 465 (190) | $^3(\pi_{II}/d–\pi^*_{II})$ | 0.7 | $\pi_{II}/d$ | 1.60[d] | $\pi^*_{VII}$ |
| | | | | | | | 1.93[d] | $\pi^*_I$ |
| **III, V** | 360 (8.0) | $^1(\pi_{III}/d–\pi^*_{III})$ | 457 (70) | $^3(\pi_{III}/d–\pi^*_{III})$ | 0.8 | $\pi_{III}/d$ | 1.85 | $\pi^*_{III}$ |
| **III, VI** | 365 (3.5) | $^1(\pi_{III}/d–\pi^*_{III})$ | 458 (50) | $^3(\pi_{III}/d–\pi^*_{III})$ | 0.7 | $\pi_{III}/d$ | 1.73 | $\pi^*_{VI}$ |
| | | | | | | | 1.93 | $\pi^*_{III}$ |
| **III, VII** | 365 (6.7) | $^1(\pi_{III}/d–\pi^*_{III})$ | 459 (30) | $^3(\pi_{III}/d–\pi^*_{III})$ | 0.9 | $\pi_{III}/d$ | 1.65 | $\pi^*_{VII}$ |
| | | | | | | | 1.88 | $\pi^*_{III}$ |
| $\{[Pd(N^N)]_2(\mu\text{-}C^N\text{-}N^C)\}^{2+}$ | | | | | | | | |
| **IV, V** | 389 (11.0) | $^1(\pi_{IV}/d–\pi^*_V)$ | 475 (43) | $^3(\pi_{IV}/d–\pi^*_V)$ | [e] | – | 1.52 | $\pi^*_V$ |
| **IV, VI** | 401 (24.6) | $^1(\pi_{IV}/d–\pi^*_I/\pi^*_V)$ | 491 (16) | $^3(\pi_{IV}/d–\pi^*_V)$ | [e] | – | 1.55 | $\pi^*_V$ |
| | | | | | | | 1.66 | $\pi^*_I$ |
| | | | | | | | 1.84[d] | $\pi^*_I$ |
| **IV, VII** | 405 (14.0) | $^1(\pi_{IV}/d–\pi^*_{II}/\pi^*_V)$ | 486 (87) | $^3(\pi_{IV}/d–\pi^*_V)$ | [e] | – | 1.56[d] | $\pi^*_V$ |
| | | | | | | | 1.68[d] | $\pi^*_{II}$ |
| | | | | | | | 1.80[d] | $\pi^*_{II}$ |

[a] $CH_3CN$, 293 K. [b] $(CH_3)_3NCO(H)–C_6H_5CH_3$, 1:1, 77 K. [c] $(CH_3)_3NCO(H)$, 293 K. [d] A current peak potential of irreversible wave at a potential scanning rate of 100 mV $s^{-1}$. [e] Distorted multielectron wave.

alongside with slightly (<200 mV) displaced reduction waves of cyclometallated ligands.

$$Rh(C^N)_2(N^N)]^+ + e^- \leftrightarrow [Rh(C^N)_2(N^N^-)],$$
$$[Pd(C^N)(N^N)]^+ + e^- \leftrightarrow [Pd(C^N)(N^N^-)].$$

The half-wave potential of the electron transfer on $\pi^*_{N^N}$-orbitals is practically independent of the nature of a cyclometallated ligand in the composition of the complex and is –(1.76±0.08) and –(1.64±0.05) V for Rh(III) and Pd(II), respectively. A small cathode shift of the potential (~100 mV) of octahedral Rh(III) complexes in relation to square-planar Pd(II) complexes with equal charges on the metal-complex fragments $\{Rh(C^N)_2\}^+$ and $\{Pd(C^N)\}^+$ can be connected with the structure of octahedral *cis*-C,C–$[Rh(C^N)_2(N^N)]^+$ complexes [17] and with increased *trans*-influence of carbanion components of cyclometallated ligands resulting in an enhanced electronic density on the diimine ligand in the *trans*-position.

Binuclear complexes $\{[Pd(N^N)]_2(\mu\text{-}C^N–N^C)\}^{2+}$ with two diimine ligands in internal spheres are characterized by three one-electron waves corresponding to the sequential reduction of a cyclometallated ligand and each of diimine ligands.

$$\{[Pd(N^N)]_2(\mu\text{-}C^N\text{-}N^C)\}^{2+} + e^- \leftrightarrow \{[Pd(N^N)]_2(\mu\text{-}C^N\text{-}N^C)^-\}^+ \quad E^1 –1.55\ V,$$

$$\{[Pd(N^N)]_2(\mu\text{-}C^N\text{-}N^C)^-]^+ + e^- \leftrightarrow \{[Pd_2(N^N)^-(N^N)](\mu\text{-}C^N\text{-}N^C)^-\} \quad E^2 –1.67\ V,$$

$$\{[Pd_2(N^N)^-(N^N)](\mu\text{-}C^N\text{-}N^C)^-\} + e^- \leftrightarrow \{[Pd(N^N)^-]_2(\mu\text{-}C^N\text{-}N^C)^-\}^- \quad E^3 –1.82\ V.$$

The close values of reduction potentials ($\Delta E$ ~150 mV) of diimine ligands in the composition of binuclear complexes point to a weak electronic interaction between them and to a rather isolated nature of $\pi^*_{N^N}$-orbitals localized on them.

In contrast to quasi-reversible nature of the ligand-centered reduction waves, the oxidation of Rh(III) complexes is characterized by irreversible waves with a current peak potential in the region of (1.04–1.32) V (Table 2). In view of the enhanced stability of Rh(III) 4*d*-orbitals in comparison with Ir(III) 5*d*-orbitals we can expect that the metal-centered Rh(III) oxidation in the composition of cyclometallated complexes should occur at a potential higher than 1.5 V [18]. Quantum-chemical calculations for the complex $[Rh(ppy)_2(N^N)]^+$[(N^N)-2,2'-bipyridinylketone and 2,2'-bipyridinylamine [19] indicate the mixed $\pi_{ppy}/d_{Rh}$ nature of HOMO of the complexes (70% $\pi_{ppy}$ and 30% $d_{Rh}$), which leads to irreversible character of their oxidation at potentials of 1.19 and 1.15 V. It allows us to assume that the complexes studied in the present work also have a similar mixed HOMO nature. Thus, unlike cyclometallated Ir(III) complexes characterized by a metal-centered MO, the reduced energy of Rh(III) 4*d* orbitals causes a significant degree of localization of MO of the complexes on the π orbital of the phenyl component of a cyclometallated ligand.

Similarly to Rh(III), the oxidation of Pd(II) complexes also is characterized by irreversible oxidation waves in the region of (0.7–1.0) V (Table 3), which also seems to be connected with the mixed $\pi_{ppy}/d_{Pd}$ nature of HOMO.

Thus, the voltammetry results show that, similarly to Ir(III) and Pt(II) complexes [20, 21], LUMO of the complexes with diimine chelating ligands $[Rh(C^N)_2\cdot(N^N)]^+$ and $[Pd(C^N)(N^N)]^+$ is localized on the $\pi^*_{N^N}$-orbital. Unlike preferentially metal-centered nature of HOMO of Ir(III) and Pt(II) complexes, HOMO of Rh(III) and Pd(II) complexes is of the mixed $\pi_{C^N}/d$ nature.

On the assumption of Koopmans theorem validity we conclude that the nature of the redox HOMO and LUMO of the complexes also defines the character of the long-wave spin-allowed optical transition of the complexes. For complexes with the ethylenediamine chelating ligand it allows us to assign the long-wave absorption band to the mixed intraligand/metal–ligand optical transition localized on the $[Rh(C^N)_2]$ and [Pd(C^N)] metal-complex fragments.

The presence of not only $\pi^*_{C^N}$, but also of $\pi^*_{N^N}$-orbitals lying lower in energy in mononuclear complexes with diimine ligands, allows us to expect a red shift of the band in relation to ethylenediamine complexes because of a lower LUMO energy. However, in the case of Rh(III) complexes, the substitution of diimines for ethylenediamine results not in the red but in the blue shift of the long-wave absorption band (Table 2). An illusory contradiction between the position of the long-wave band in absorption spectra of Rh(III) complexes and the position of $\pi^*_{N^N}$- and $\pi^*_{C^N}$-orbitals is caused by a low effectiveness of overlapping HOMO ($\pi_{C^N}/d$) and LUMO ($\pi^*_{N^N}$) orbitals [19] resulting in a low oscillator strength of the optical transition between them. It results in overlapping the optical transition between HOMO and LUMO with more high-energy and more intensive transition between HOMO and [LUMO + 1] ($\pi^*_{C^N}$). The participation of $\pi^*_{C^N}$-orbitals of cyclometallated ligands in the long-wave optical transition of complexes is confirmed by the correlation of the band energy and the difference in the potentials of oxidation and ligand-centered reduction of complexes with the participation of $\pi^*_{C^N}$-orbitals (Fig. 1).

Similarly to Rh(III) complexes, electronic absorption spectra of $[Pd(C^N)(N^N)]^+$ complexes (Table 3) are also characterized by one wide long-wave $\pi_{C^N}/d$–$\pi^*_{C^N}$-band of the intraligand/metal–ligand charge transfer transition, whereas preferentially metal-centered character of HOMO of Ir(III) and Pt(II) complexes causes [20, 21] the presence of two long-wave $d$–$\pi^*_{N^N}$ charge transfer metal–ligand bands and of $d$–$\pi^*_{C^N}$ bands displaced to blue side.

Unlike spin-allowed optical transitions, the character of spin-forbidden transitions defining phosphorescent properties of complexes depends not only on the energy sequence of orbitals, but also on the singlet-triplet energy splitting, the values of which for the states of the intraligand transition and of the ligand–ligand and metal–ligand charge-transfer are different. Inversely proportional dependence of the "extra stabilization" energy of the triplet excited state term on the effective electron phototransfer distance [22] is connected with a decrease in the the "extra stabilization" energy in the series of states: intraligand transition > ligand–ligand charge transfer > metal–ligand charge transfer, and with the nature of the lowest in energy triplet excited state responsible for phosphorescence of complexes, which depends on the energy gap between singlet states of the metal–ligand

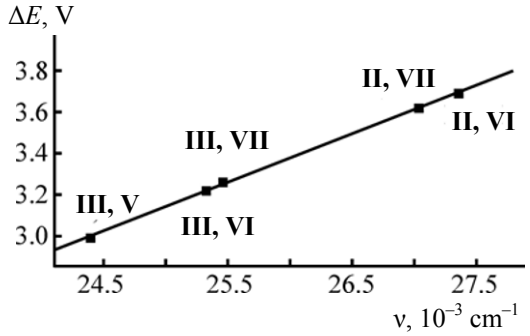


**Fig. 1.** Effect of ligands on the difference ($\Delta E$) in potentials of ligand-centered $\pi^*_{C\wedge N}$ reduction and oxidation of $[Rh(C\wedge N)_2(N\wedge N)]^+$ complexes and on the frequency ($\nu$) of the long-wave absorption band maximum.

and ligand–ligand charge transfer and of the intraligand transition.

In accordance with the enhanced energy of the π*-orbital of 1-phenylpyrazole, the luminescence of its Rh(III) and Pd(II) complexes with ethylenediamine is displaced into the UV region (<400 nm) outside the spectral sensitivity of the instrument.

Close energy positions of vibration-structured ($\nu_{vibr}$ ~1400 $cm^{-1}$) low-temperature luminescent spectra and rather prolonged duration (0.32–7.9 ms) of its exponential decay for Rh(III) complexes with 1-phenylpyrazole and diimine ligands (Table 2), as compared with phosphorescence of free diimines, allow us to assign their luminescence to the intraligand spin-forbidden $\pi_{N\wedge N}$–$\pi^*_{N\wedge N}$ optical transition.

The replacement of phenyl-substituted pyridine and pyrimidine for cyclometallated 1-phenylpyrazole, along with the decrease in the energy gap between $\pi^*_{N\wedge N}$- and $\pi^*_{C\wedge N}$-orbitals, results in sequential red displacement (~700 and ~1100 $cm^{-1}$) of the phosphorescence spectrum of complexes with diimine ligands and in a decrease in time of its quenching (~200 and ~10 μs). It allows us to assign phosphorescence of these complexes to the process of radiative degradation of excitation energy from the mixed state of the ligand–ligand/metal–ligand charge transfer ($\pi_{C\wedge N}/d$–$\pi^*_{N\wedge N}$) (Fig. 2). In accordance with the increase in the HOMO energy, the substitution of ethylenediamine for diimine chelating ligands is accompanied by a red shift (~900 $cm^{-1}$) of the phosphorescence spectrum of Rh(III) complex with 4,6-diphenylpyrimidine as a result of the ligand-metal–ligand charge transfer optical transition ($\pi_{C\wedge N}/d$–$\pi^*_{C\wedge N}$).

The substitution of diimines for ethylenediamine results in the vibration-structured low-temperature luminescence of Pd(II) complexes (Table 2), the energy position (~476 nm) and decay time (43–22 μs) of which allow us to assign it to the mixed spin-forbidden optical transition with the ligand–ligand/metal–ligand charge transfer ($\pi_{C\wedge N}/d$–$\pi^*_{N\wedge N}$). The wavelengths of luminescent spectra of the complexes with phenyl-substituted pyridine and pyrimidine (462–465 and 457–459 nm) depend only slightly on the chelating ligand nature. Red shift of the spectra (~1700 $cm^{-1}$) relative to the phosphorescence spectra of free ligands H(C^N) (Table 1) points to the mixed nature of the optical transition with the ligand/metal–ligand charge transfer ($\pi_{C\wedge N}/d$–$\pi^*_{C\wedge N}$) responsible for the phosphorescence of the complexes (Fig. 3).

In spite of the similarity of LUMOs ($\pi^*_{C\wedge N}$–$\pi_{C\wedge N}$) for the complexes with ethylenediamine and diimine chelating ligands $\{[Pd(N\wedge N)]_2(\mu$–C^N–N^C$)\}^{2+}$, the closeness of energies of LUMO and $\pi^*_{N\wedge N}$ orbitals of diimine ligands, and the difference in energies of the singlet-triplet splitting of the states of intraligand transition and ligand–ligand and metal–ligand charge transfer result in a change in the nature of the excited state responsible for phosphorescence of the complexes with diimines compared to the ethylenediamine complex. We assigned the phosphorescence of the binuclear complex with ethylenediamine to the radiation energy degradation from the state of the intraligand transfer/metal–ligand charge transfer ($\pi^*_{C\wedge N}$–$\pi_{C\wedge N}/d$–$\pi^*_{C\wedge N}$–$\pi_{C\wedge N}$), whereas for the complexes with diimine ligands, from the state of the ligand–ligand/metal–ligand charge transfer ($\pi^*_{C\wedge N}$–$\pi_{C\wedge N}/d$–$\pi^*_{N\wedge N}$).

In contrast to Ir(III) and Pt(II)complexes, for Rh(III) and Pd(II) complexes the phosphorescence is observed only in frozen (77 K) solutions and is completely quenched in liquid solutions at room temperature. The effective temperature quenching of phosphorescence of Rh(III) and Pd(II) complexes can be assigned to thermally activated transfer of photoexcitation energy on metal-centered *d*–*d** excited states, which suffer radiationless deactivation [23].

The global estimate of the obtained data shows that the model of localized molecular orbitals is applicable to the description of electrochemical and optical properties of cyclometallated complexes $[Rh(C\wedge N)_2\cdot(N\wedge N)]^+$, $[Pd(C\wedge N)(N\wedge N)]^+$, and $\{[Pd(N\wedge N)]_2(C\wedge N$–$N\wedge C)\}^{2+}$ with ethylenediamine and diimine chelating ligands. In comparison with 5*d*-platinum metals Ir(III)

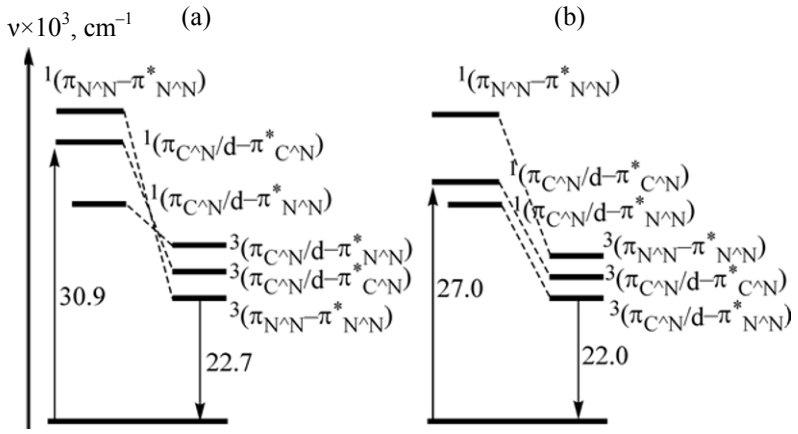


**Fig. 2.** Qualitative diagram of changes in the energy of the lowest singlet and triplet excited states for Rh(III) complexes based on (a) 1-phenylpyrazole and (b) 2-phenylpyridine (**II**) with 2,2'-bipyridine.

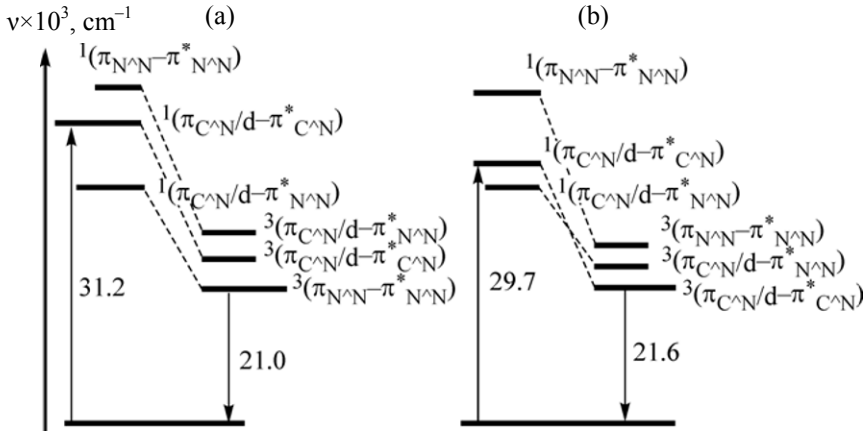


**Fig. 3.** Qualitative diagram of changes in the energy of the lowest singlet and triplet excited states for Pd(II) complexes based on (a) 1-phenylpyrazole and (b) 2-phenylpyridine (**II**) with 2,2'-bipyridine.

and Pt(II), the complexes of Rh(III) and Pd(II) are characterized by a series of special features. Unlike the metal-centered character of HOMO of Ir(III) and Pt(II) complexes, HOMO of Rh(III) and Pd(II) complexes is of the mixed phenyl-metal ($\pi_{C^\wedge N}/d$) nature. Owing to a low effectiveness of HOMO and LUMO overlapping ($\pi^*_{N^\wedge N}$) in the complexes with diimine ligands it results not only in irreversible character of oxidation voltammograms, but also in the appearance of a long-wave absorption band with participation of LUMO and more high-energy $\pi^*_{C^\wedge N}$-orbitals. In comparison with the luminescence of Ir(III) and Pt(II) complexes caused by a metal–ligand charge-transfer transition, the character of the spin-forbidden optical transition responsible for the low-temperature phosphorescence of Rh(III) and Pd(II) complexes with diimine ligands is defined by the ratio of the energy gap between localized $\pi^*_{N^\wedge N}$- and $\pi^*_{C^\wedge N}$-orbitals and by the energy of singlet–triplet splitting of the intraligand transition and ligand–ligand charge-transfer states.

## EXPERIMENTAL

Complexes of Rh(III) and Pd(II) were prepared by the procedures [24–26]. The electronic absorption spectra were recorded at room temperature on an SF-2000 spectrophotometer in acetonitrile solutions. The luminescence study was carried out on a KSVU-1 installation with a pulse laser photoexcitation (LGI-21, λ 337 nm, $\tau_{imp}$ 10 ns) at 77 K in vitreous templates $(CH_3)_3NCO(H)$–$C_6H_5CH_3$ (1:1) [27]. Voltammograms were obtained on an SVA-1B installation at 293 K in a three-electrode cell with separated working spaces with (Pt), auxiliary (glassgraphite), and reference (Ag) electrodes in the presence of 0.1 M $[N(C_4H_9)_4]BF_4$ solution in $(CH_3)_3NCO(H)$ [28]. Potentials were

measured in relation to the ferrocenium–ferrocene redox system at a potential scanning rate of 100 mV $s^{-1}$.

## REFERENCES


1. Koo, C.-K., Wong, K.-L., Man, C.W.-Y., Lam, Y.-W., So, L.K.-Y., Tam, H.-L., Tsao, S.-W., Cheah, K.-W., Lau, K.–C., Yang, Y.-Y., Chen, J.–C., and Lam, M.H.-W., *Inorg. Chem*., 2009, vol. 48, no. 3, p. 872.
2. Borisov, S.M. and Climant, I., *Anal. Chem*., 2007, vol. 79, no. 19, p. 7501.
3. Williams, J.A.G., Delay, S., Rochester, D.L., and Murphy, L., *Coord. Chem. Rev*., 2008, vol. 252, nos. 23–24, p. 2596.
4. Dupont, J., Consorti, C.S., and Spencer, J., *Chem. Rev*., 2005, vol. 105, no. 6, p. 2527.
5. Aiello, I., Dattilo, D., Ghedini, M., and Golemme, A., *J. Am. Chem. Soc*., 2001, vol. 123, no. 23, p. 5598.
6. Chakraborty, S., Wadas, T.J., Hester, H., Schmehl, R., and Eisenberg, R., *Inorg. Chem*., 2005, vol. 44, no. 20, p. 6865.
7. Thompson, M.E., Djurovich, P.I., Barlow, S., and Marder, S., *Comprehensive Organometal. Chem. III.,* 2007, vol. 12, p. 101.
8. DeArmond, M. and Carlin, C., *Coord. Chem. Rev*., 1985, vol. 63, p. 325.
9. Koopmans, T., *Physics*, 1933, vol. 1, no. 1, p. 104.
10. Maestri, M., Sandrini, D., Balzani, V., Maeder, U., and von Zelewsky, A., *Inorg. Chem*., 1987, vol. 26, no. 8, p. 1323.
11. Demas, J.N., *J. Chem. Educ.,* 1983, vol. 60, no. 10, p. 803.
12. Gas, B., Klima, J., Zalis, S., and Vlcek, A.A., *J. Electroanal. Chem*., 1987, vol. 222, no. 1, p. 161.
13. Sandrini, D., Maestri, M., Ciano, M., Maeder, U., and von Zelewsky, A., *Helv. Chim. Acta*, 1990, vol. 73, no. 5, p. 1306.
14. Maestri, M., Sandrini, D., Balzani, V., Maeder U., and von Zelewsky, A., *Inorg. Chem*., 1987, vol. 26, no. 8, p. 1323.
15. Hill, R.H. and Puddephatt, R.J., *J. Am. Chem. Soc*., 1985, vol. 107, no. 5, p. 1218.
16. Ohsawa, Y., Sprouse, S., King, K.A., DeArmond, M.K., Hanck, K.W., and Watts, R.J., *J. Phys. Chem*., 1987, vol. 91, no. 5, p. 1047.
17. Steel, P.J., *J. Organomet. Chem*., 1991, vol. 408, no. 3, p. 395.
18. Calagero, G., Giuffrida, G., Seroni, S., Ricevuto, V., and Campagna, S., *Inorg. Chem*., 1995, vol. 34, no. 3, p. 541.
19. Su, L., Yu, Y.C., Tseng, M.C., Wang, S.P., and Huang, W.L., *Dalton Trans*., 2007, no. 31, p. 3440.
20. Lamansky, S., Djurovich, P., Murthy, D., Abdel-Razzaq, F., Lee, H.-F., Adachi, C., Burrows, P.E., Forest, S.R., and Thompson, M.E., *J. Am. Chem. Soc*., 2001, vol. 123, no. 18, p. 4304.
21. Ivanova, E.V., Puzyk, M.V., and Balashev, K.P., *Zh. Obshch. Khim.,* 2009, vol. 79, no. 10, p. 1600.
22. Busby, M., Matousek, P., Towrie, M., Clark, I.P., Motevalli, M., Hartl, F., and Vlcek, A., *Inorg. Chem*., 2004, vol. 43, no. 14, p. 4523.
23. Barigelletti, F., Sandrini, D., Maestri, M., Balzani, V., von Zelewsky A., Chassot, L., Joliet, P., and Maeder, U., *Inorg. Chem*., 1988, vol. 27, no. 20, p. 3644.
24. Ivanova, E.V. and Balashev, K.P., *Zh. Obshch. Khim*., 2009, vol. 79, no. 10, p. 1749.
25. Ivanova, E.V. and Balashev, K.P., *Zh. Obshch. Khim*., 2009, vol. 79, no. 10, p. 1756.
26. Ivanova, E.V., Puzyk, M.V., and Balashev, K.P., *Opt. Spektr*., 2009, vol. 106, no. 3, p. 409.
27. Vasil'ev, V.V., Balashev, K.P., and Shagisultanova, G.A., *Opt. Spektr*., 1983, vol. 54, no. 5, p. 876.
28. Vasil'ev, V.V., Balashev, K.P., and Shagisultanova, G.A., *Opt. Spektr*., 1983, vol. 54, no. 5, p. 876.
29. Kotlyar, V.S. and Balashev, K.P., *Elektrokhim*., 1996, vol. 32, no. 11, p. 1358.